Spectroscopic and Theoretical Studies of [Fe(CO)₃(1,4-diaza-1,3-butadiene)] Complexes; X-Ray Structure and Magnetic Circular Dichroism and Resonance-Raman Spectra of [1,2-Bis(2',6'-di-isopropylphenylimino)ethane-NN']tricarbonyliron †

Maarten W. Kokkes, Derk J. Stufkens,* and Ad Oskam
Anorganisch Chemisch Laboratorium, University of Amsterdam, J. H. van 't Hoff Instituut,
Nieuwe Achtergracht 166, 1018 WV Amsterdam, The Netherlands

The X-ray structure of the title compound has been determined by the heavy-atom method and refined by means of block-diagonal least-squares calculations from 5 537 independent reflections. The crystals are monoclinic, space group $P2_1/n$, with unit-cell dimensions $a = 18.422(4)$, $b = 16.155(3)$, $c = 9.966(3)$ Å, $\beta = 90.40(3)°$, and $Z = 4$. The final R value was 0.044. The compound has a distorted square pyramidal structure with Fe–N bond lengths of 1.929(2) and 1.926(3) Å. Molecular-orbital (m.o.) calculations reveal a low-lying lowest unoccupied molecular orbital which has substantial $\pi^*(\alpha\text{-di-imine})$ character. Most low-lying transitions are directed to this orbital. M.c.d., electronic absorption, and resonance-Raman (r.R.) spectra, obtained by excitation into the lowest electronic absorption bands, are reported. They give evidence for several electronic transitions in the low-lying absorption band. Two of these transitions are pseudo-degenerate, leading to an A term in the m.c.d. spectrum. The r.R. spectra are very weak which means that the bonds of the complex are hardly affected by the charge-transfer transitions. The spectra show that the complex relaxes to another conformation in the excited state. Differences between the m.o. calculations and the r.R. spectra are discussed.

During the last few years much attention has been paid in our laboratory to the resonance-Raman (r.R.) and electronic absorption spectra of low-valence transition-metal α-di-imine complexes. For the complexes [M(CO)₄L] (L = α-di-imine; M = Cr, Mo, or W) and [Ru(CO)₃L] the r.R. spectra gave information about the character of the metal to α-di-imine charge-transfer (c.t.) transitions and about the properties of the lowest excited state in relationship to the photochemical behaviour.[1-4] In fact, a qualitative relationship appeared to exist for the [M(CO)₄L] complexes between the relative r.R. intensity of $\nu_{sym}(CO)_{cis}$ and the photosubstitution quantum yield of the cis carbonyl ligands by phosphines upon irradiation into the metal to α-di-imine c.t. transitions.[3] The corresponding [Fe(CO)₃L] complexes also show rather high quantum yields for the photosubstitution of a carbonyl ligand, a property which has been reported quite recently by Johnson and Trogler.[5] In order to explain this behaviour we studied the r.R. spectra and metal-to-ligand charge-transfer (m.l.c.t.) photochemistry of this type of complexes.

In this paper we report the electronic absorption, magnetic circular dichroism (m.c.d.), and r.R. spectra of two representative complexes. Furthermore, the X-ray structure of one of these complexes is presented together with molecular-orbital (m.o.) calculations for a model compound. In a forthcoming article we shall report the photochemistry in solution and in matrices at 10 K. For the complexes under study the α-di-imine ligand is a 1,4-diaza-1,3-butadiene, RN=CH–CH=NR. Since only those complexes are stable in which the 1,4-diaza-1,3-butadiene possesses a bulky substituent at the co-ordinating nitrogen atoms, we used 1,2-bis(2',6'-di-isopropylphenylimino)ethane (bdpie) and 1,2-bis(di-isopropylmethylimino)ethane (bdmie).

Experimental

The ligands and d^8 complexes were synthesized according to published methods[6-8] {Found: C, 67.45; H, 7.00; N, 5.45. Calc. for [Fe(CO)₃(bdpie)]: C, 67.45; H, 7.05; N, 5.35. Found: C, 58.1; H, 8.70. Calc. for [Fe(CO)₃(bdmie)]: C, 58.15; H, 8.20%}.

All samples were dissolved in freshly distilled and deoxygenated solvents and prepared with standard inert-gas techniques in a glove-box because of the photochemical sensitivity of the complexes towards oxygen and water.

Resonance-Raman spectra were measured on a Jobin Yvon HG2S Ramanor spectrophotometer. The Raman spectra were excited by a SP model 171 argon-ion laser and a CR 490 tunable dye laser with Rhodamine 110, the sodium salt of fluorescein, Stilbene 3, and Coumarin 6 in ethylene glycol as dyes, and with cyclo-octatetraene as photosensitizer. An Anaspec 300-S with a bandpass of 0.4 nm was used as a premonochromator. The spectra were recorded with a spinning cell. Band intensities were measured with a Hewlett-Packard model 10 calculator and corrected for the sensitivity of the spectrophotometer by a curve based on the Stokes–anti-Stokes relationship of the band of methylene chloride at 284 cm⁻¹, as described by Montero et al.[9] and corrected for ν^4.

Electronic absorption spectra were measured on a Cary 14 spectrophotometer and i.r. spectra on a Nicolet 7199B FT-IR interferometer with a liquid-nitrogen-cooled Hg, Cd, Te detector. M.c.d. spectra were recorded at the Laboratorium voor Algemene Chemie of the Rijksuniversiteit van Utrecht on a home-made instrument. The concentrations were chosen such that the optical density was about 0.75. The spectra were measured with a bandpass of 3 nm at a magnetic field strength of 7.0 T and were corrected for the baseline. Gaussian curve analyses were carried out on a Du Pont model 310 curve resolver.

Molecular-orbital calculations were performed with the CNDO/S method in the parametrization of del Bene and Jaffé[10] for C, H, N, and O and Louwen[11] for Fe, in which the repulsion integrals were approximated by the method of Nishimoto and Mataga.[12]

Crystal-structure Determination of [Fe(CO)₃(bdpie)].—*Crystal data.* C₂₉H₃₆FeN₂O₃, $M = 516.45$, Monoclinic, space
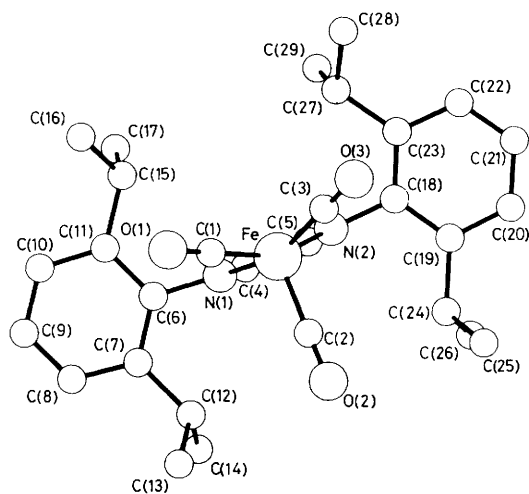
Figure 1. ORTEP drawing of [Fe(CO)₃(bdpie)]

Table 2. Bond lengths (Å) and angles (°) with e.s.d.s in parentheses

Fe–N(1)	1.929(2)	N(2)–C(5)	1.330(5)
Fe–N(2)	1.926(3)	N(2)–C(18)	1.439(4)
Fe–C(1)	1.788(4)	C(1)–O(1)	1.145(5)
Fe–C(2)	1.800(4)	C(2)–O(2)	1.144(5)
Fe–C(3)	1.789(3)	C(3)–O(3)	1.141(5)
N(1)–C(4)	1.328(4)	C(4)–C(5)	1.390(5)
N(1)–C(6)	1.444(4)		

N(1)–Fe–N(2)	80.1(1)	Fe–N(1)–C(6)	128.5(2)
N(1)–Fe–C(1)	90.9(2)	Fe–N(2)–C(5)	115.4(2)
N(1)–Fe–C(2)	105.3(1)	Fe–N(2)–C(18)	127.9(3)
N(1)–Fe–C(3)	158.4(1)	C(4)–N(1)–C(6)	116.0(3)
N(2)–Fe–C(1)	155.9(2)	C(5)–N(2)–C(18)	116.6(3)
N(2)–Fe–C(2)	107.2(1)	N(1)–C(4)–C(5)	114.1(3)
N(2)–Fe–C(3)	91.0(1)	N(2)–C(5)–C(4)	114.3(3)
C(1)–Fe–C(2)	96.8(2)	Fe–C(1)–O(1)	179.2(4)
C(1)–Fe–C(3)	89.4(1)	Fe–C(2)–O(2)	178.6(4)
C(2)–Fe–C(3)	96.1(2)	Fe–C(3)–O(3)	179.0(3)
Fe–N(1)–C(4)	115.5(2)		

Table 1. Final co-ordinates with estimated standard deviations (e.s.d.s) in parentheses

Atom	x	y	z	Atom	x	y	z
Fe	0.229 44(2)	0.008 02(2)	0.013 28(3)	C(13)	0.333 0(3)	0.137 5(4)	−0.368 6(6)
O(1)	0.128 8(2)	−0.028 1(2)	−0.208 3(3)	C(14)	0.355 1(3)	0.251 9(4)	−0.204 0(7)
O(2)	0.363 2(2)	−0.035 0(2)	−0.130 8(4)	C(15)	0.061 4(2)	0.153 8(3)	−0.010 4(4)
O(3)	0.203 5(2)	−0.158 9(2)	0.117 5(3)	C(16)	−0.008 9(3)	0.114 5(4)	−0.059 5(7)
N(1)	0.216 5(1)	0.125 5(1)	−0.012 2(3)	C(17)	0.047 3(3)	0.224 7(4)	0.087 8(6)
N(2)	0.257 3(1)	0.047 2(2)	0.188 7(2)	C(18)	0.277 4(2)	−0.001 2(2)	0.304 3(3)
C(1)	0.168 2(2)	−0.013 5(2)	−0.122 2(3)	C(19)	0.350 3(2)	−0.021 2(2)	0.327 2(3)
C(2)	0.311 6(2)	−0.017 4(2)	−0.074 3(4)	C(20)	0.367 3(2)	−0.067 6(2)	0.440 9(4)
C(3)	0.213 5(2)	−0.093 6(2)	0.078 0(3)	C(21)	0.314 5(3)	−0.093 5(3)	0.528 6(4)
C(4)	0.238 4(2)	0.172 9(2)	0.089 2(3)	C(22)	0.243 1(2)	−0.074 2(2)	0.503 9(3)
C(5)	0.261 4(2)	0.129 0(2)	0.201 7(3)	C(23)	0.221 9(2)	−0.028 2(2)	0.391 0(3)
C(6)	0.184 7(2)	0.168 2(2)	−0.125 5(3)	C(24)	0.410 3(2)	0.006 0(3)	0.232 5(4)
C(7)	0.229 0(2)	0.194 3(2)	−0.232 0(3)	C(25)	0.453 9(3)	−0.067 4(4)	0.180 9(6)
C(8)	0.195 4(3)	0.238 3(2)	−0.335 7(3)	C(26)	0.458 7(3)	0.071 4(4)	0.300 6(7)
C(9)	0.122 4(3)	0.254 8(2)	−0.335 0(4)	C(27)	0.142 9(2)	−0.004 9(3)	0.368 2(4)
C(10)	0.079 7(2)	0.226 8(2)	−0.231 7(4)	C(28)	0.091 0(3)	−0.074 4(4)	0.408 8(5)
C(11)	0.109 1(2)	0.182 9(2)	−0.124 6(3)	C(29)	0.123 2(3)	0.074 8(4)	0.441 8(5)
C(12)	0.309 6(2)	0.176 1(2)	−0.236 3(3)				

group $P2_1/n$, $a = 18.422(4)$, $b = 16.155(3)$, $c = 9.966(3)$ Å, $\beta = 90.40(3)°$, $U = 2\,965.9$ Å³, $D_c = 1.156$ g cm⁻³, $Z = 4$, $F(000) = 1\,069$, $\lambda(\text{Mo}–K_\alpha) = 0.7107$ Å, $\mu(\text{Mo}–K_\alpha) = 5.34$ cm⁻¹, crystal size $0.5 \times 0.25 \times 0.32$ mm.

5 537 Reflections with $I > 2.5\,\sigma(I)$ were measured on a Nonius CAD 4 diffractometer (θ—2θ range) using graphite-monochromated Mo-K_α radiation. No absorption correction was applied. The crystal structure was determined by means of the heavy-atom method. The hydrogen atoms were located in a ΔF synthesis. Refinement was carried out by means of block-diagonal least-squares calculations, anisotropic for Fe, C, N, and O and isotropic for H. The final R value was 0.044. A weighting scheme $w = (1.1 + F_o + 0.01\,F_o^2)^{-1}$ was applied [13] and the anomalous scattering of Fe was taken into account. The calculations were performed with the X-RAY system [14] and PLUTO. [15] The final co-ordinates are listed in Table 1, selected bond distances and angles in Table 2.

Results and Discussion

Figure 1 shows an ORTEP picture of the compound [Fe(CO)₃-(bdpie)]. The structure resembles that of [Fe(CO)₃(MeN=N–N=NMe)] [16] which was described as a distorted square pyramid. The Fe–N distance of 1.929(2) Å is longer than in the

tetra-azadiene compound (1.83 Å), due to the weaker back-bonding of the α-di-imine ligand. Strong π backbonding has also been reported for [Ni-(RN=N–N=NR)₂] (R = C₆H₃Me₂-3,5), in which the Ni–N distance is 1.85 Å, whereas in the structurally related [Ni-{(C₆H₁₁)N=CH–CH=N(C₆H₁₁)}₂] the Ni–N distance is 1.92 Å. [18] In the present compound the Fe atom is located 0.163(3) Å above the plane formed by the N–C–C–N moiety [standard deviation of the four atoms making up the plane (σ) = 0.001]. For [Fe(CO)₃(MeN=N–N=NMe)] on the other hand a planar FeN₄ moiety is found. This different bonding behaviour is caused by the fact that the α-di-imine, which has polarized bonds in contrast to the tetra-azadiene ligand, has a higher electron density at the N atom which therefore partly loses its sp_z character. As a result the Fe atom will be lifted out of the plane formed by the N–C–C–N moiety. This polarization also explains the better σ-donor ability of the α-di-imine compared with the tetra-azadiene ligand.

The crystal structure of tricarbonyl(pyridine-2-diphenyl-carbaldimine)iron determined by Frühauf [19] more closely resembles a distorted trigonal bipyramid. Because the electronic properties of these compounds differ from those of the diaza-butadiene complexes they are also being studied in our laboratory and will be discussed in a forthcoming article.

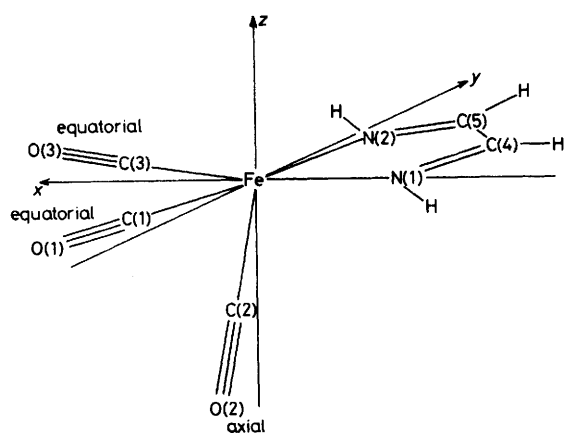In the present compound the steric influence of the isopro-

Figure 2. Structure and choice of axes of [Fe(CO)₃(HN=CH–CH=NH)]
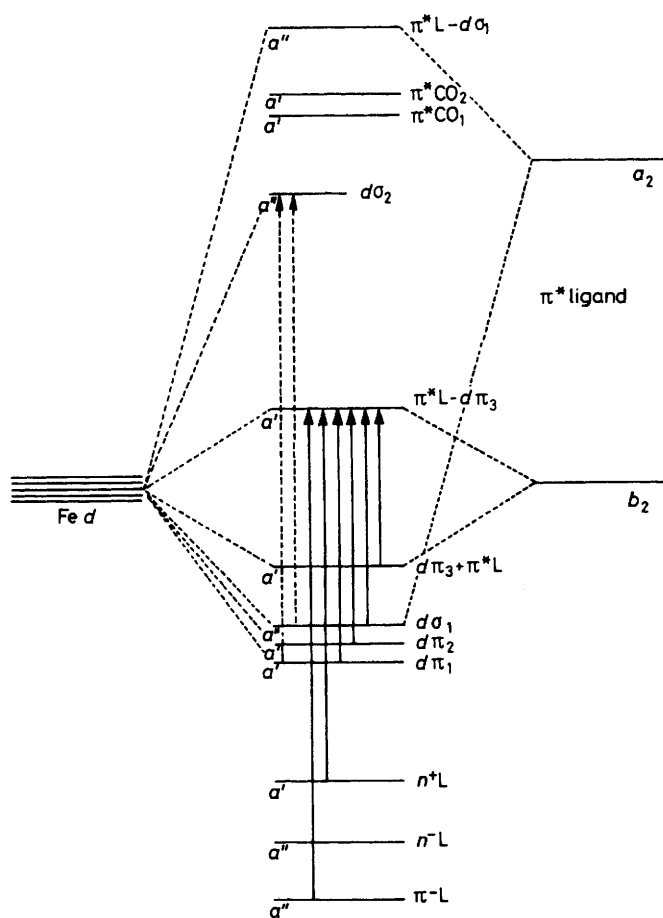
Figure 3. Relevant part of the m.o. scheme and observed transitions

Figure 4. Electronic absorption (a) and m.c.d. (b) spectrum of [Fe(CO)₃(bdpie)] in iso-octane

pyl groups is clearly seen in Figure 1. These groups shield the nitrogen atom where the π^* orbital has its highest electron density and therefore increase the stability of the complex.

CNDO/S and restricted Hartree-Fock (r.H.F.) Calculations for [Fe(CO)₃(HN=CH–CH=NH)].—A CNDO/S calculation for the ground state and restricted Hartree-Fock CNDO/S calculations for the excited states were performed for the model compound [Fe(CO)₃(HN=CH–CH=NH)]. Atomic co-

ordinates were taken from the corresponding [Fe(CO)₃(bdpie)], in which the aryl substituent was replaced by an H atom, positioned 1.0 Å from the N atom and in the same direction as the phenyl C atom (see Figure 2).

The calculated m.o. diagram is presented in Figure 3. Just as for [Fe(CO)₃(MeN=N–N=NMe)],[20] a low-lying lowest unoccupied molecular orbital (l.u.m.o.) exists which has substantial π^*L character (L = HN=CH–CH=NH). Most low-lying electronic transitions are directed to this orbital. We calculated the excited states for the first four transitions as well as for the $(d\pi_3 + \pi^*L \rightarrow \pi^*CO_1)$ and the $(d\sigma_1 \rightarrow d\sigma_2)$ (ligand-field) transitions. The intraligand transitions $(n^+L \rightarrow \pi^*L - d\pi_3)$ and $(\pi^-L \rightarrow \pi^*L - d\pi_3)$ did not convèrge. Calculated bond orders, localized electron populations, and state energies are given in Tables 3 and 4. The first four transitions are directed from Fe d orbitals towards the l.u.m.o. From these the highest occupied molecular orbital (h.o.m.o.) $\rightarrow$l.u.m.o. transition $(d\pi_3 + \pi^*L \rightarrow \pi^*L - d\pi_3)$ is clearly metal–ligand bonding→antibonding, whereas the next three transitions originate from orbitals having more Fe d character.

It should be noted that for the calculation of the excited state belonging to the $(d\pi_2 \rightarrow \pi^*L - d\pi_3)$ transition the interaction between the n^+ lone pair and the Fe d orbitals has not been taken into full account, so the energy of this state might be higher. In the u.v. photoelectron spectra of [Fe(CO)₃L] complexes [21] the $d\pi_2$ orbital is also found at higher energy than the $d\sigma_1$ and $d\pi_1$ orbitals which nearly coincide. Furthermore, the absolute values of the r.H.F. calculated states are not reliable as expected for a semiempirical method. In C_s

Table 3. Some calculated bond orders in the ground state and various excited states

	Bond order						
Electronic transition	Fe–C(1,3) *	Fe–C(2)	Fe–N(1,2)	C(1,3)–O(1,3)	C(2)–O(2)	C(4)–C(5)	N–C(4,5)
Gound state	0.467	0.442	0.450	2.351	2.345	1.274	1.582
$d\pi_3 + \pi^*L \rightarrow \pi^*L - d\pi_3$	0.495	0.457	0.314	2.148	2.166	1.358	1.391
$d\sigma_1 \rightarrow \pi^*L - d\pi_3$	0.475	0.359	0.323	2.150	2.192	1.389	1.374
$d\pi_2 \rightarrow \pi^*L - d\pi_3$	0.438	0.422	0.318	2.163	2.168	1.380	1.381
$d\pi_1 \rightarrow \pi^*L - d\pi_3$	0.456	0.367	0.321	2.157	2.184	1.378	1.383
$d\pi_3 + \pi^*L \rightarrow \pi^*CO$	0.437	0.466	0.257	1.937	2.119	1.176	1.737
$d\sigma_1 \rightarrow d\sigma_2$	0.495	0.477	0.422	2.106	2.132	1.308	1.536

* Fe–C(1,3) represents the averaged value of Fe–C(1) and Fe–C(3).

Table 4. Some calculated energies (in atomic units) and electron populations for the ground state and various excited states

		Localized electron population						
Electronic transition	Energy	Fe	C(1,3) *	C(2)	N(1,2)	O(1,3)	O(2)	C(4,5)
Ground state	−316.8448	7.74	3.86	3.86	5.21	6.17	6.16	3.98
$d\pi_3 + \pi^*L \rightarrow \pi^*L - d\pi_3$	−316.7585	7.46	3.72	3.72	5.34	6.31	6.31	3.99
$d\sigma_1 \rightarrow \pi^*L - d\pi_3$	−316.7340	7.47	3.72	3.72	5.34	6.30	6.30	3.99
$d\pi_2 \rightarrow \pi^*L - d\pi_3$	−316.7317	7.47	3.71	3.73	5.34	6.30	6.31	3.99
$d\pi_2 \rightarrow \pi^*L - d\pi_3$	−316.7306	7.48	3.71	3.73	5.35	6.30	6.30	3.99
$d\pi_3 + \pi^*L \rightarrow \pi^*CO$	−316.7053	7.51	3.90	3.75	5.16	6.40	6.33	3.92
$d\sigma_1 \rightarrow d\sigma_2$	−316.6630	7.58	3.76	3.74	5.24	6.34	6.32	3.98

* C(1,3) represents the averaged value of C(1) and C(3).

Figure 5. Electronic absorption spectrum of [Fe(CO)₃(bdmie)] in iso-octane

Table 5. Electronic absorption spectral data (cm⁻¹) ^{a} for some [Fe(CO)₃L] complexes in benzene

Complex	$10^{-3}\sigma$(c.t.)	$10^{-3}\sigma$(i.l.) ^{b}	$10^{-3}\sigma$(l.f.)	$10^{-3}\sigma$(i.l.) ^{b}
[Fe(CO)₃(bptie)]	19.7 (4.0)	27.0 (sh)		
[Fe(CO)₃(bdpie)]	20.0 (4.6)	25.8 (4.2)	33.3 (sh)	
[Fe(CO)₃(bdmie)]	20.1 (5.9)	26.9 (3.0)	32.2 (sh)	40.0 (sh)
Ligand				
bptie		28.1		
bdpie		28.0		
bdmie		34.6		

^{a} $10^{-3}\varepsilon_{max}$. (dm³ mol⁻¹ cm⁻¹) given in parentheses. ^{b} i.l. = Intraligand.

symmetry all possible transitions are allowed, but by assuming local C_{2v} symmetry for the intraligand transitions the ($n^-L \rightarrow \pi^*L - d\pi_3$) transition will be forbidden and by assuming local C_{3v} symmetry for the ligand-field transitions which, as will be shown below, is a good approximation, the ($d\pi_2 \rightarrow d\sigma_2$) and ($d\pi_3 + \pi^*L \rightarrow d\sigma_2$) transitions will be forbidden.

Electronic Absorption and M.C.D. Spectra.—The electronic absorption spectrum of [Fe(CO)₃(bdpie)] shown in Figure 4(a)

consists of two bands in the visible region. On the basis of the m.o. calculations the lowest-energy band is assigned to transitions between the Fe d and α-di-imine π^* orbitals. This band however, hardly shows any solvatochroism, which means that the corresponding transitions have no c.t. character. This is also evident from the weak r.R. effects observed for the α-di-imine stretching modes as will be discussed later. The energies of these transitions will therefore mainly be determined by overlap stabilization. Although four transitions are allowed, the band at 500 nm is broad and shows no structure even at lower temperatures. It will be shown below that the m.c.d. spectrum and the r.R. excitation profiles reveal the presence of these transitions.

The band at 388 nm is assigned to an intraligand transition ($n^+L \rightarrow \pi^*L - d\pi_3$). Just as for [W(CO)₄(bptie)] [bptie = 1,2-bis(p-tolylimino)ethane], this transition is red shifted with respect to the free ligand.[4] Furthermore, the spectrum shows a shoulder at 300 nm, which can better be observed for [Fe(CO)₃(bdmie)] and which is assigned to a ligand-field (l.f.) transition (see Figure 5). For [Fe(CO)₃(bdmie)] a shoulder is observed at 250 nm, which may belong to the ($\pi^-L \rightarrow \pi^*L - d\pi_3$) transition. The energies and intensities of these bands are collected in Table 5.

The m.c.d. spectrum of [Fe(CO)₃(bdpie)] is shown in Figure 4(b). The magnetic circular dichroism can be expressed in terms of the molecular parameters A, B, and C according to

Table 6. Carbonyl-stretching modes (cm⁻¹), measured in pentane

v(CO)	[Ru(CO)₃(bmie)] *	[Fe(CO)₃(bdpie)]	[Fe(CO)₃(bptie)]	[Fe(CO)₃(bdmie)]
a	2 055	2 041	2 038	2 026
a'	1 988	1 973	1 976	1 955
a''	1 975	1 967	1 965	1 946

* bmie = 1,2-Bis(mesitylimino)ethane.

Table 7. Resonance-enhanced α-di-imine ligand modes of [M-(CO)₃L] complexes; w = weak, m = medium, and s = strong. All spectra taken in benzene

Vibrational mode	Raman wavenumbers (cm⁻¹)		
	[Ru(CO)₃(bmie)] *	[Fe(CO)₃(bdpie)]	[Fe(CO)₃(bdmie)]
v_{sym}(M−N)	200w	220w	250w
v(M−C)	334m	378m	420m
	377m	415m	453s
δ(M−C−O)	453s	494s	475m
	472s	553m	500s
	508m	617m	563s
δ(M−L)	533s	702w	725s
	842s	869m	910m
v_{sym}(CN)	1 490w	1 476w	1 495m
v(CO)	not observed	1 973w	1 950w
		2 032w	2 030w

* Values from ref. 4.

$\theta_M = -21.3458 \{f_1A + f_2[B + (c/kT)]\}$; θ_M represents the molar ellipticity per unit magnetic field and f_1 and f_2 are frequency functions, describing the shape of the absorption bands.[22,23] A transition to a degenerate state gives rise to a m.c.d A term, a transition from a degenerate state to a C term. For molecules having no degenerate states, only B terms will be observed, which arise from the mixing of levels by the magnetic field. This will be the case for the complexes under study which have merely C_s symmetry. The lowest-energy absorption band corresponds with a m.c.d. term which can be resolved in three B terms by Gaussian analysis. These three transitions also fit the corresponding band in the absorption spectrum and correspond to three maxima in the r.R. excitation profiles, as will be shown below. The presence of three instead of four different transitions may be due to the fact that two d levels nearly or completely coincide (see below).

The second absorption band shows a single B term, in agreement with the assignment of this band to a single $(n^+L \rightarrow \pi^*L - d\pi_3)$ transition. A remarkable m.c.d. effect is observed for the l.f. transition at about 300 nm. This transition corresponds to an A term in the m.c.d. spectrum although the complex has merely C_s symmetry. Apparently, this transition is governed by a higher symmetry of the metal d levels, which is evident from the occurrence of only three transitions in the lowest-energy band (see above) and from the near coincidence of the $a'(d\pi_1)$ and $a''(d\sigma_1)$ levels in the m.o. diagram (see Figure 3). The symmetry of these d levels will mainly be determined by the carbonyl groups. According to the crystal structure and to the carbonyl-stretching region in the i.r. spectrum (see Table 6), the Fe(CO)₃ moiety has merely C_s symmetry. However, two CO stretching modes nearly coincide, which means that the deviation from C_{3v} symmetry is only small, which may explain the presence of the A term in the m.c.d. spectrum. The m.c.d. spectrum of [Fe(CO)₃(bdmie)] closely resembles that of [Fe(CO)₃(bdpie)] although the m.c.d. effects are smaller. The l.f. transition is observed for both compounds at almost the same energy.
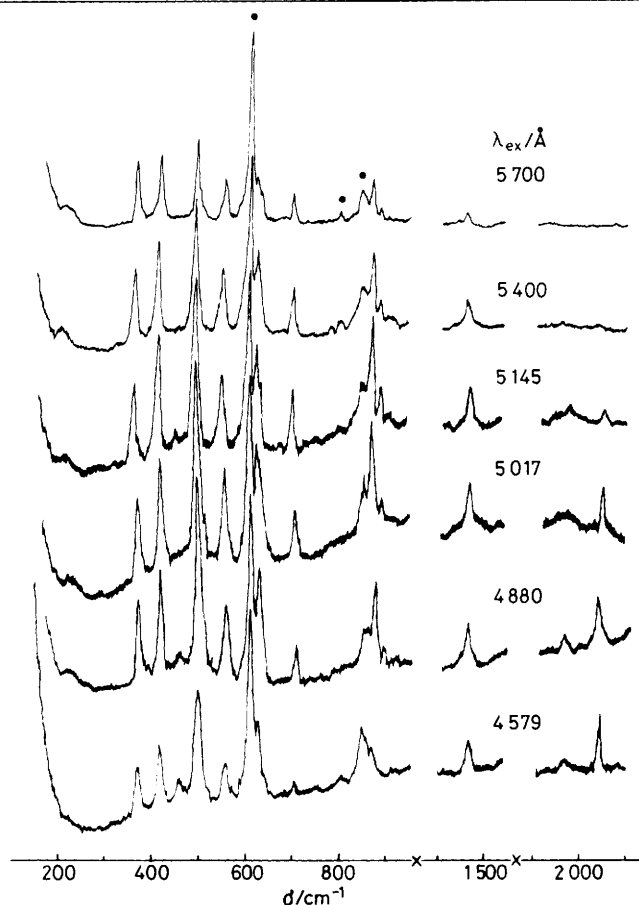
Resonance-Raman Spectra.—Relatively weak r.R. effects

Figure 6. Resonance-Raman spectra of [Fe(CO)₃(bdpie)] upon excitation at different wavelengths in benzene. Solvent bands are indicated with a filled circle

are observed for the [Fe(CO)₃L] complexes. The spectra had to be taken from solutions with an optical density of 15.5, whereas for the corresponding [M(CO)₄L] (M = Cr, Mo, or W) complexes the optical density of the solutions was about 2.5.[1-4] Although, the r.R. effects are weak the emission will be due to Franck-Condon or A-term scattering, since excitation takes place into strongly allowed electronic transitions.[24] Such weak r.R. effects are observed when the equilibrium conformation of a molecule hardly changes on going from the ground state to the excited state. This is in accordance with the results from the m.o. calculations for this complex (see above) and for the corresponding tetra-azadiene compound.[20] All bands are polarized,with the exception of one at 469 cm⁻¹, and they have a depolarization ratio, $\rho = 1/3$. The r.R. spectra of [Fe(CO)₃(bdpie)], measured at different wavelengths, are depicted in Figure 6, while the wavenumbers of the vibrational modes and their assignments are presented in Table 7. Predominantly low-frequency bands are observed belonging to v_{sym}(M−N), v(M−C), and δ(M−C−O) vibrations. The r.R. effect of v_{sym}(C−N) of the α-di-imine ligand at 1 476 cm⁻¹ is

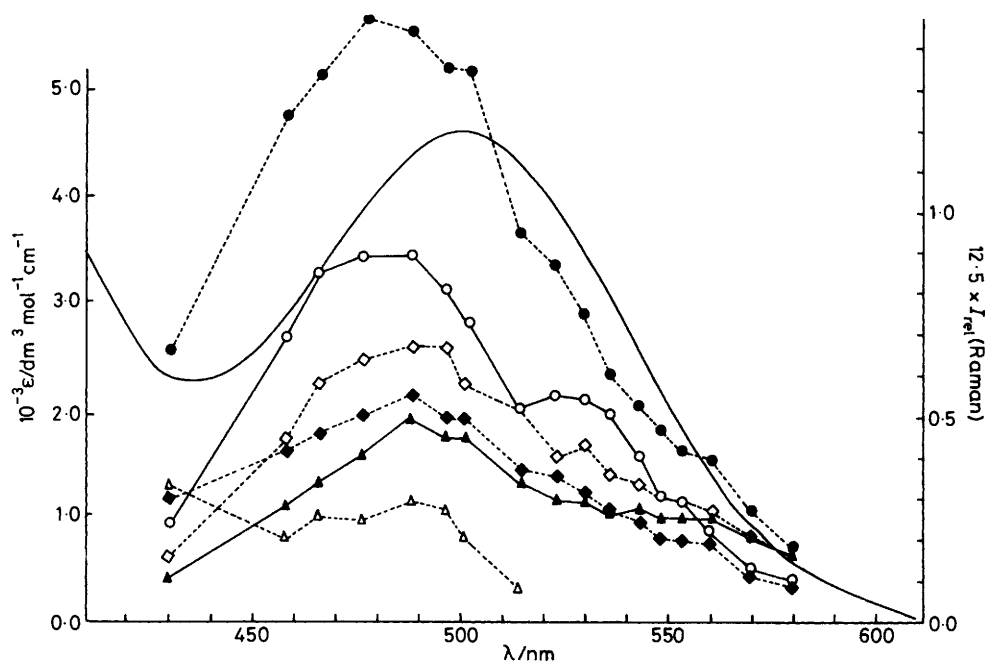**Figure 7.** Excitation profiles of carbonyl vibrational modes of [Fe(CO)₃(bdpie)] in benzene, relative to the band of this solvent at 992 cm⁻¹. Modes: ▲, v(FeC) 378 cm⁻¹; ◇, v(FeC) 415 cm⁻¹; ●, δ(FeCO) 494 cm⁻¹; ◆, δ(FeCO) 553 cm⁻¹; ○, δ(FeCO) 617 cm⁻¹; △, v(CO) 2 032 cm⁻¹
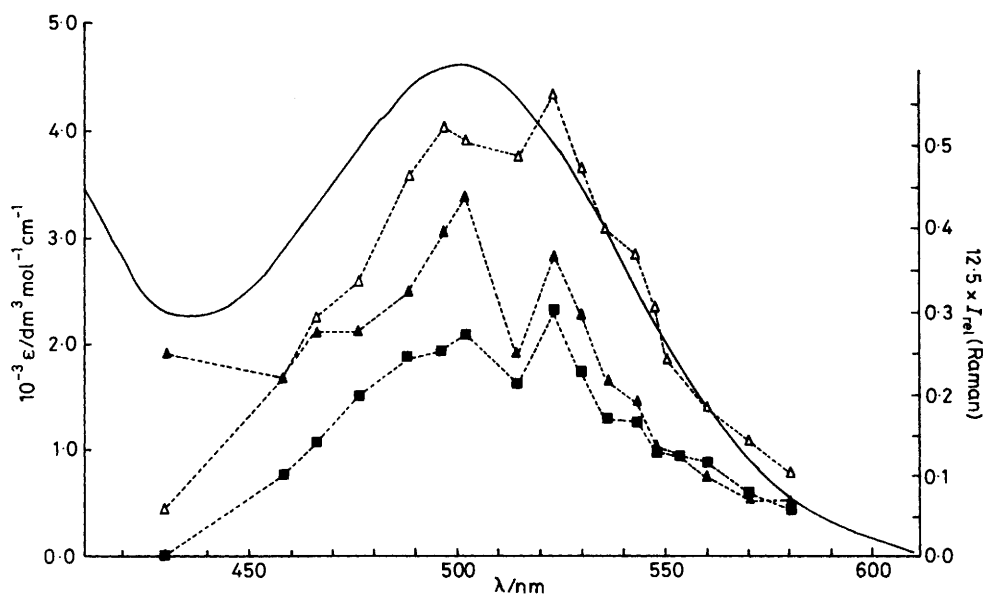

Figure 8. Excitation profiles of ligand vibrational modes of [Fe(CO)₃(bdpie)] in benzene, relative to the band of this solvent at 992 cm⁻¹. Modes: ■, δ(FeL) 702 cm⁻¹; △, δ(FeL) 869 cm⁻¹; ▲, v_{sym}(CN) 1 476 cm⁻¹

very weak, which means that the metal–ligand bands are more affected by the electronic transitions than are the α-di-imine bands. This result is in agreement with our observations that these transitions have no c.t. character.

A r.R. effect is observed for two other α-di-imine vibrations, at 702 and 869 cm⁻¹ respectively. Since these bands are also observed for [Fe(CO)₃(bdmie)], which possesses an aliphatic α-di-imine, they are assigned to bending modes of the $\overline{\text{FeNCCN}}$ moiety, instead of to vibrations of the substituted aryl rings at the co-ordinating nitrogen atoms.[4]

Upon excitation at the high-energy side of the absorption band at 500 nm, an extra depolarized band is observed at 469 cm⁻¹ which is assigned to an asymmetric (a″) v(M–C) vibration. Contrary to the [M(CO)₄L] complexes, only a weak r.R. effect is observed for the band in the CO-stretching region at 2 032 cm⁻¹. This band is assigned to the stretching vibration of the axial carbonyl because it disappears upon substitution of this ligand.[25] For the tetracarbonyl compounds the r.R. effect of v_{sym}(CO)$_{cis}$ has been explained by a through-space overlap between π* orbitals of the α-di-imine ligand and cis carbon-

yls.[2,3] For steric reasons such an overlap cannot occur for the [Fe(CO)₃L] complexes, which explains the weak r.R. effect of ν(CO). Finally a very weak r.R. effect is observed for the symmetrical stretching mode of the equatorial carbonyls at 1 973 cm⁻¹.

Excitation Profiles.—The r.R. excitation profiles of the most Raman-active vibrations are shown in Figures 7 and 8. No reliable profile could be obtained for ν_{sym}(FeN) at 220 cm⁻¹, because this band is very weak and partly obscured by the Raleigh scattering. All intensities were related to the intensity of the band of the solvent benzene at 992 cm⁻¹, The excitation profiles of ν_{sym}(CN) and of two bending modes of the $\overline{\text{FeNCCN}}$ moiety (Figure 8) show the presence of two maxima at about 500 and 525 nm respectively. The positions of these maxima agree with the maxima derived by Gaussian analysis from the absorption and m.c.d. spectra. A third maximum is observed in the excitation profiles of the ν(FeC), δ(FeCO), and ν(CO) vibrations (Figure 7). This maximum, which also coincides with the position of a shoulder in the absorption and m.c.d. spectra, is rather broad, indicating the presence of two nearly coincident electronic transitions. According to these excitation profiles, mainly vibrations of the $\overline{\text{FeNCCN}}$ moiety are coupled to the two lowest-energy transitions, which will therefore be $d\pi_3 + \pi^*L \rightarrow \pi^*L - d\pi_3$ and $d\pi_2 \rightarrow \pi^*L - d\pi_3$ respectively. The broad maximum in the excitation profiles between 450 and 500 nm now apparently belongs to one or two transitions, mainly localized on the Fe(CO)₃ moiety, since only vibrations of this group are reasonably r.R. active. This maximum is tentatively assigned to the nearly coincident transitions $d\sigma_1 \rightarrow \pi^*L - d\pi_3$ and $d\pi_1 \rightarrow \pi^*L - d\pi_3$.

For ν_{sym} (CN) and ν(CO) a pre-resonance-Raman effect for the intraligand transition ($n^+L \rightarrow \pi^*L - d\pi_3$) is observed. The weak r.R. effects observed for this complex agree with the small differences in calculated bond orders between the ground and excited states (see Table 3). According to Table 3 the largest r.R. effect is expected for ν_{sym}(FeN) because the order of the Fe–N bond changes the most, on going to the excited states. This is, however, not observed. On the contrary, the band belonging to ν_{sym}(FeN) is one of the weakest bands in the r.R. spectra. This result may be connected with the observation of strong r.R. effects for several bending modes of the complex with respect to the stretching vibrations. This means that electronic excitation has a greater influence on the bond angles of the complex than on the bond lengths. Apparently, the complex relaxes in the excited states to a more stable conformation with slightly different bond angles. This is not accounted for in the calculations and may therefore explain the discrepancy between the calculations and the r.R. spectra with respect to the behaviour of the Fe–N bonds. It is evident from the weak r.R. effects that no metal–ligand bonds are severely affected by any of the electronic transitions within the absorption band. Photosubstitution of CO, which is observed with rather high quantum yields for these complexes (*e.g.* photosubstitution of CO by PPh₃ in [Fe(CO)₃(bdpie)] upon irradiation at 5 145 Å gives a quantum yield $\phi_p{}^i = 0.18$),[4,25] cannot therefore be the result of a primary photoprocess involving dissociative loss of CO in the excited state. The same conclusion has been drawn by Johnson and Trogler[5] from calculated changes of bond orders for the corresponding tetra-azadiene complexes. However, as mentioned above, results from calculations for these complexes have to be used with care because of possible relaxation of the excited states to a more stable conformation.

References

1 R. W. Balk, D. J. Stufkens, and A. Oskam, *Inorg. Chim. Acta*, 1978, **28**, 133.
2 R. W. Balk, D. J. Stufkens, and A. Oskam, *Inorg. Chim. Acta*, 1979, **34**, 267.
3 R. W. Balk, T. Snoeck, D. J. Stufkens, and A. Oskam, *Inorg. Chem.*, 1980, **19**, 3015.
4 R. W. Balk, D. J. Stufkens, and A. Oskam, *J. Chem. Soc., Dalton Trans.*, 1982, 275.
5 C. E. Johnson and W. C. Trogler, *J. Am. Chem. Soc.*, 1981, **103**, 6352.
6 H. Bock and H. tom Dieck, *Chem. Ber.*, 1967, **100**, 228.
7 S. Otsuka, T. Yoshida, and A. Nakamura, *Inorg. Chem.*, 1967, **6**, 20.
8 H. tom Dieck and A. Orlops, *Angew. Chem.*, 1975, **87**, 246.
9 S. Montero, D. Bermejo, and M. A. Lopez, *Appl. Spectrosc.*, 1976, **30**, 628.
10 J. del Bene and H. H. Jaffé, *J. Chem. Phys.*, 1968, **48**, 1807.
11 J. N. Louwen, personal communication.
12 K. Nishimoto and N. Mataga, *Z. Phys. Chem. (Frankfurt am Main)*, 1957, **12**, 325.
13 D. W. J. Cruickshank and D. A. Lilling in ' Computing Methods and the Phase Problem in *X*-RAY Crystal Analysis,' Pergamon, Oxford, 1961, p. 45.
14 J. M. Stewart, The *X*-RAY system, Technical Report TR 446, Computer Science Center, University of Maryland, College Park, Maryland, 1976.
15 W. D. S. Motherwell, PLUTO, Program for plotting crystal and molecular structures, University of Cambridge, 1976.
16 R. J. Doedens, *Chem. Commun.*, 1968, 1271.
17 P. Overbosch, G. van Koten, and O. Overbeek, *J. Am. Chem. Soc.*, 1980, **120**, 2091.
18 H. tom Dieck, M. Svoboda, and T. Greiser, *Z. Naturforsch.*, *Teil B*, 1981, **36**, 823.
19 H. W. Frühauf, Habilitationsschrift, University of Duisburg, W. Germany, 1980, pp. 41, 42.
20 W. C. Trogler, C. E. Johnson, and D. E. Ellis, *Inorg. Chem.*, 1981, **20**, 980.
21 J. N. Louwen and A. Oskam, unpublished work.
22 P. J. Stephens, *J. Chem. Phys.*, 1970, **52**, 3489.
23 P. N. Schatz and A. J. McCaffery, *Q. Rev., Chem. Soc.*, 1969, **23**, 552.
24 R. J. H. Clark and B. Stewart, *Struct. Bonding (Berlin)*, 1979, **36**, 1.
25 M. W. Kokkes, D. J. Stufkens, and A. Oskam, unpublished work.